The behavior of Al, Mn, Ba, Sr, REE and Th isotopes during in vitro degradation of large marine particles

R. Arraes-Mescoff, M. Roy-Barman, L. Coppola, M. Souhaut, K. Tachikawa, C. Jeandel, Richard Sempere, C Yoro

The behavior of Al, Mn, Ba, Sr, REE and Th isotopes during in vitro degradation of large marine particles

R. Arraes-Mescoff [a], M. Roy-Barman [a,*], L. Coppola [a], M. Souhaut [a], K. Tachikawa [a,1], C. Jeandel [a], R. Sempéré [b], C. Yoro [b]

[a] *LEGOS / UMR 5566, 14 Avenue Edouard Belin, 31400 Toulouse, France*
[b] *LMM, CNRS / INSU, Campus de Luminy, F13288 Marseille Cedex 9, France*

Received 29 September 1999; received in revised form 1 May 2000; accepted 17 July 2000

Abstract

The extent and the time constant of dissolution of a set of inorganic tracers during the decomposition of large marine particles are estimated through in vitro experiments. Large marine particles were collected with in situ pumps at 30 m and 200 m in the Ligurian Sea at the end of summer. They were subsequently incubated under laboratory conditions with their own bacterial assemblage for 20 days in batches under oxic conditions in the dark. Some samples were initially sterilized in order to observe possible differences between biotic and abiotic samples. Particulate (> 0.2 μm) and dissolved (< 0.2 μm) concentrations of Al, Sr, Ba, Mn, Rare Earth Elements (REE) and Th isotopes were determined over time. We obtain percentages of dissolution in agreement with the general knowledge about the solubility of these tracers: Th ≈ Al < Heavy REE < Light REE < Mn < Ba < Sr. For Mn and Ce, precipitation/adsorption occurs at the end of the experiment probably due to their oxidation as insoluble oxides. Particulate residence time of the tracers ranged from less than 1 day to 10–14 days. During the experiment, biological activity has a control on the dissolution process through the remineralization of particulate organic carbon. In the 30 m experiment, the observed dissolution of aragonite indicates that the pH of the incubation solution significantly decreases in response to the CO_2 respiration. Speciation calculations suggest that this pH shift leads to a decrease of the complexation of dissolved REE by carbonate ions. Th isotope data are consistent with an irreversible dissolution of Th and they do not support a rapid particle–solution chemical equilibrium.

Keywords: Marine particles; Dissolution; Trace elements; Thorium isotopes; Western Mediterranean Sea

1. Introduction

Large (> 50 μm) marine particles play a key role in the biogeochemical cycle of the elements in the ocean. These particles have mainly a biological origin (organic flocculate, fecal pellets) and they represent the main transport pathway between the surface water and the sediment. When they sink toward the

* Corresponding author. Tel.: +33-561332988; fax: +33-561253205.
E-mail address: matthieu.barman@cnes.fr (M. Roy-Barman).
[1] Present address: CEREGE, Europole de l'Arbois, BP 80, 13545 Aix en Provence, France.

sediment, they interact with seawater and small suspended particles through physical, chemical and biological processes such as aggregation–disaggregation, dissolution–precipitation, biodegradation, adsorption–desorption (Lal, 1977). These processes modify the chemical composition of the particles and therefore the fluxes of settling matter (Schaffer, 1996). Various types of models have been developed to quantify these processes (McCave, 1975; Bacon and Anderson, 1982; Murnane et al., 1994; Ruiz-Pino, 1994). They can be calibrated with thorium data (Bacon and Anderson, 1982) or laboratory experiments (Balistrieri et al., 1981). However, they are still poorly constrained due to the large number of processes involved and the lack of data for many of them.

This work is a part of the Etude Intégrée des Métaux En Trace dans l'Océan (EIMETO) project to study the interactions between the various phases in the oceanic water column (seawater, colloids, small and large particles). Our aim is to use in vitro experiments to constrain the dissolution of large marine particles in response to bacterial activity. These experiments were accomplished by a collaboration between marine geochemists and marine biologists to study the possible coupling between biological activity and the behavior of organic and inorganic tracers. In this paper, we present the results obtained for the inorganic tracers. Results obtained for organic tracers and bacterial production are presented elsewhere (Yoro, 1998).

To estimate the extent and the time constant of dissolution of a set of inorganic tracers, we have collected marine particles at 30 m and 200 m in the Ligurian Sea. Aliquots of these particles were incubated for different times at constant temperature and then the incubation solutions and the residual particles were analyzed. We have selected a set of tracers that are useful to understand the transport of matter in the ocean. Aluminum (Al) is a tracer of the lithogenic fraction in the particulate matter (Davies and Buat-Ménard, 1990; Guerzoni et al., 1997). Strontium (Sr) is a tracer of biogenic particulate phases. It is found in carbonates and in acantharian (planktonic protozoan) tests that are made of celestite ($SrSO_4$, Bernstein et al., 1992). Barium (Ba) is a tracer of exported production (Dehairs and Goeyens, 1987a; Francois et al., 1995). The behaviors of Sr and Ba have similarities, but celestite is much more soluble than barite ($BaSO_4$). Manganese (Mn) is sensitive to redox conditions (Sunda et al., 1983; Moffett, 1997). Formation of Mn oxyhydroxides induces the scavenging of other trace metals (Balistrieri et al., 1981; Tachikawa et al., 1999b) and is mediated by bacterial activity (Moffett, 1994). Rare Earth Elements (REE) and the isotopic composition of Neodymium (Nd) are used as tracers of water masses and seawater/particle interactions (Jeandel et al., 1995; Henry et al., 1994; Tachikawa et al., 1999a). Thorium (Th) is an insoluble element with isotopes of distinct origins (Roy-Barman et al., 1996, 2000). In situ produced Th isotopes are commonly used to calibrate particle related processes (Bacon and Anderson, 1982).

2. Sampling and analytical procedure

2.1. Sampling

The samples were collected at the end of summer at the "DYnamique des Flux Atmosphériques en MEDiterranée" (DYFAMED) site, 5 nautical miles (9 km) off Nice in the Ligurian Sea (Fig. 1). The site is located in a coastal environment and it receives strong eolian inputs. Large particles were collected by filtration of seawater (17 m^3 at 30 m and 23 m^3 at 200 m) on Teflon grids (diameter: 142 mm, pore size 60 μm) with in situ pumps (Challenger Oceanic). The particulate matter was shared approximately equally between organic and inorganic analyses. We also sampled seawater at 200 m with Niskin bottles. This water was filtered through 0.2 μm filters to remove bacteria and grazers. Counting by epifluorescence microscopy after DAPI staining (Porter and Feig, 1980) indicated that 0.2 μm filtration was an efficient protocol to remove living microorganisms such as flagellates and bacteria. This filtered water was used for particle removal and dilution. Therefore, we assume that marine particles have been degraded mainly by their own bacterial assemblage. For the 30 m samples, optical observations indicated the presence of pteropods and Scanning Electron Microscope (SEM) observations indicated the presence of a majority of diatoms and of some coccolithophorids. For the 200 m samples, optical observations indicated the presence of small crustaceans and

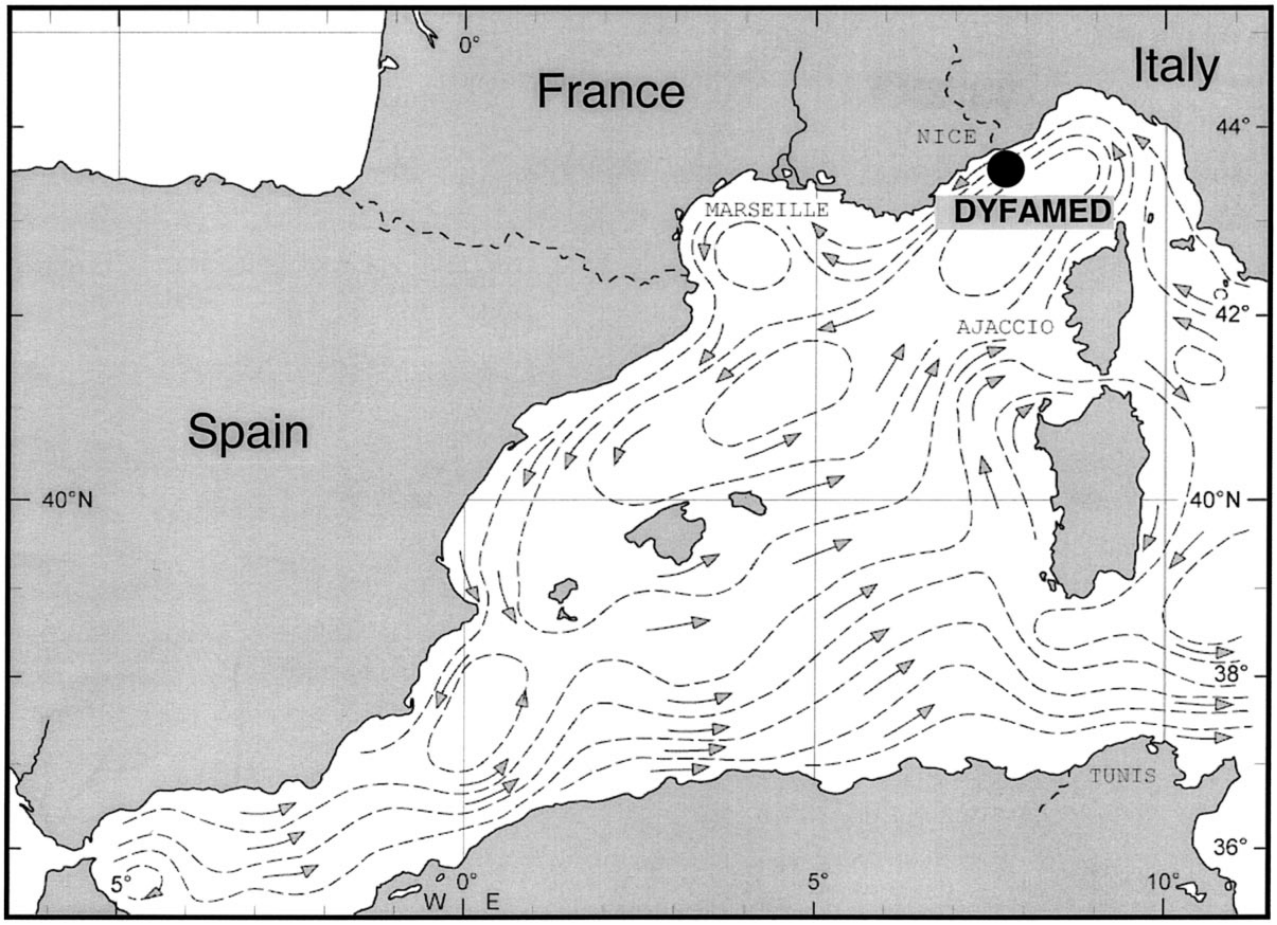

Fig. 1. Sampling site location.

SEM observations indicated the presence of diatoms and silicoflagellates.

2.2. Incubation procedure

A detailed description of the protocol is given elsewhere (Sempéré et al., 2000). Immediately after sampling, the largest swimmers were removed from the filters. Then filters were maintained wet by adding few cubic centimeters of 0.2 μm filtered seawater and stored for 24 h in the dark at 4°C to minimize bacterial activity until the beginning of the incubation experiments in the laboratory. In Marseille laboratory, the particles were removed from the filters by rinsing the filters with 0.2 μm filtered seawater. Particles were distributed in 500-cm^3 polypropylene bottles using a high precision peristaltic pump (Perfifill IQ 2000, Jencons) while the initial solution was continuously stirred. Each subsample is formed by a large number (> 100) of 2 cm^3 doses supplied by a silicone tubing (Heussner et al., 1990). Experimental error calculated from the variability ($n = 6$) of GF/F-particulate organic carbon (POC) at the initial time in different bottles after particle dispatching were within 4%. The volume of the solution was adjusted to 200–250 cm^3 with 0.2-μm filtered seawater. During the separation procedure, the bottles were maintained in ice in order to reduce bacterial activity. Particles from 200 m were separated in eight aliquots (hereafter referred as C series): each aliquot contains particles filtered from approximately 1.4 m^3 of seawater. Particles from 30 m were separated in 10 aliquots: each aliquot contains particles filtered from approximately 0.79 m^3 of seawater (hereafter referred as D series).

After separation, the bottles were placed in incubators at in situ temperature (23 ± 1°C for the 30 m

samples and 13 ± 1°C for the 200 m samples) and in the dark to prevent photosynthesis. The bottles were gently agitated upside down once a day. Available oxygen in the incubation bottles was calculated from the total organic carbon (TOC) consumption and from the volume of available air in the incubation bottle. It indicates that the experiments were conducted under aerobic conditions. The bacterial growth was measured as bacterial production using leucine incorporation technique (Kirchman et al., 1993). The total bacterial production in the incubation solutions was much larger than in seawater due to the strong particle enrichment. Each bacterium has the activity (organic matter consumption, reproduction) of a typical marine bacterium whose development is not limited by food (at least at the beginning of the incubation). Some samples were initially sterilized in order to observe possible differences between biotic and abiotic samples (C7 was poisoned with sodium azide; D5 and D9 were sterilized by ^{60}Co-gamma irradiation of 16 kGy for 2 h). In these bottles, bacterial growth was negligible. Incubations lasted up to 21 days and were stopped by separating the incubation solution from the residual particles. This was done by filtration on 0.2 μm Durapore filters. The incubation time "t" represents the time between the end of the particle sub-sampling with the particle separator and the end of the incubation. The maximum incubation time roughly corresponds to the large particle transit time in the water column of the Western basin of the Mediterranean Sea: large particles have a sinking speed of 100 m/day for a depth of 2000 m yielding to a transit time of 20 days (Fowler et al., 1987; Henry et al., 1994).

2.3. Chemical analysis

2.3.1. Incubation solutions

For Al, Ba, Mn and Sr, a small aliquot (1.4 cm^3) of the incubation solution was diluted in 20 cm^3 of 2% HNO_3 and an Indium–Rhenium internal standard was added to the diluted solution. The diluted solution was analyzed by ICP-MS (ELAN 5000, Perkin Elmer, see Valladon et al., 1995).

The remaining solution was used for Th and REE analysis. ^{229}Th, ^{150}Nd and ^{174}Yb spikes and Fe carrier were added to the solution. After a week of isotopic equilibration, the pH was raised to 8–9 using NH_3 to produce $Fe(OH)_3$. The precipitate was recovered by centrifugation, dissolved in HNO_3 and processed through anionic ion exchange column (AG1X8) to separate Th from Fe + REE. Th was further purified (Chen et al., 1987; Roy-Barman et al., 1996) and run by Thermal Ionization Mass Spectrometry (Finnigan Mat 261 equipped with a Spectromat post-counting system). The Fe + REE fraction was dried and then dissolved in 0.5 cm^3 of 6 N HCl. This solution was passed through an anionic ion exchange column (0.5 cm^3 of AG1X8) that fixed Fe and let the REE pass through. REE were eluted completely with 2.5 cm^3 of 6 N HCl. The yield of the REE chemistry was $> 80\%$. Purified REE were diluted in 10 cm^3 of 2% HNO_3, Indium–Rhenium internal standard was added to the solution and the sample was analyzed by ICP-MS (ELAN 6000, Perkin Elmer).

2.3.2. Particles

The 0.2 μm filters were placed in a hot 5% HCl solution for a day to detach the particles. The particles were washed out from the filter with distilled water. Then, the particles were dissolved in 1 cm^3 of *aqua regia*. The solution was dried and the residue was dissolved again in 0.3 cm^3 of 16 N HNO_3. The sample was centrifuged to separate the solution from the residual solids. Residual solids were dissolved in $HF–HNO_3–HClO_4$, dried and dissolved in 16 N HNO_3. When complete dissolution of these solids was achieved (no residual solid after centrifugation), the supernatant solution and the sink solution were mixed back together. This procedure allowed to use HF for the residual solid dissolution without producing CaF_2 precipitates with the Ca released during the 5% HCl and *aqua regia* dissolution steps. The final solution was separated in two splits. One aliquot was dried, diluted in 20 cm^3 of 2% HNO_3, Indium–Rhenium internal standard was added and the sample was analyzed for Al, Ba, Mn, Sr and REE by ICP-MS (ELAN 6000, Perkin Elmer). The second aliquot was dried, ^{229}Th spike was added and the sample was processed through anionic ion exchange resin to separate Th from the matrix (Chen et al., 1987; Roy-Barman et al., 1996). Purified Th was run by Thermal Ionization Mass Spectrometry.

2.4. Blanks

In order to estimate the reagent contribution and the possible contamination during the incubation, 0.2 μm filtered seawater (200 m) was incubated with no prior addition of particles. This water was filtered after incubation and both filtered solutions (later referred as "seawater blanks") and filters (later referred as "particle blanks") were analyzed. For particles, the blank contribution is $\leq 1\%$ for Al at 30 m and $\leq 23\%$ for Al at 200 m, $\leq 4\%$ for Ba, below detection limit for Mn, below detection limit for REE except for La ($\leq 30\%$) and Ce ($\leq 40\%$) at 200 m, $\leq 7\%$ for Th at 30 m and $\leq 44\%$ for Th at 200 m. For Sr it ranges from 5% to 40%. The particulate concentrations presented in this study are blank-corrected. Concentrations in seawater blanks were similar to Mediterranean seawater for all elements indicating no significant contamination except Al and Th (see discussion below).

2.5. Accuracy

Accuracy of the ICP-MS analysis was checked by running the SLRS standard (Institute for Environmental Chemistry, Ottawa) and a standard solution (ICP-MS grade). Agreement between ICP-MS measurements and recommended values of Al, Ba, Sr, Mn, REE and Th is typically better than 7%. Accuracy for Th measurement by TIMS was checked by running Th standards. Agreement between measurements and the recommended $^{230}Th/^{232}Th$ value (Banner et al., 1990) is typically better than 2%.

3. Results

Unless stated otherwise, the concentrations of elements in the filtered incubation solutions and in the residual particles are expressed in 10^{-9} g of element per gram of incubation solution (ng/g). Results are given in Tables 1–3.

For both series, concentrations in the initial incubation solutions (D0–D1 and C0) are systematically higher than in the seawater blanks indicating that dissolution had started before the beginning of the incubation during the 24 h between the particle pumping and the separation of the different aliquots. Therefore, in the following, we will consider the evolution of concentrations since the time $t = -24$ h (that is when the particles have been collected). This allows us to maintain a timescale which is consistent with the organic tracer study (Yoro, 1998).

At 30 m, concentrations in incubation solutions (23–28 ng/g for Ba, 3.6–7.1 ng/g for Mn, 8734–9236 ng/g for Sr) are systematically higher than in seawater blanks except for Al (4.7–23 ng/g). At 30 m, concentrations on the residual particles are: 552–1382 ng/g for Al, 10–21 ng/g for Ba, 4.5–10 ng/g for Mn, 9–80 ng/g for Sr. At 200 m, concentrations in incubation solutions (16–26 ng/g for Ba, 2.5–4.3 ng/g for Mn, 8000–8300 ng/g for Sr) are significantly higher than in seawater blanks except for Al (8.6–16.4 ng/g) and Sr (8000–8300 ng/g). At 200 m, concentrations on the residual particles are: 23–113 ng/g for Al, 2.5–4.3 ng/g for Ba, 0.6–3.5 ng/g for Mn, 5–15 ng/g for Sr.

Ba (11.2–12.5 ng/g) and Sr (8225–8277 ng/g) concentrations in seawater blanks are similar to those of Mediterranean seawater (Bernat et al., 1972). REE concentrations in seawater blanks are in good agreement with Mediterranean seawater (Greaves et al., 1991; Henry et al., 1994). Mn concentrations (1.9–2.1 ng/g) in seawater blanks are higher than values reported for Mediterranean seawater (0.03–0.11 ng/g, Morley et al., 1997). However, our samples were collected only 9 km from the shore whereas Morley's samples were collected at offshore sites. Strong concentration gradients are commonly observed between coastal area and open waters (Landing and Bruland, 1987). ^{232}Th concentrations (0.27–0.33 pg/g) of seawater blanks are higher than the concentrations measured on the same seawater that has not followed the incubation procedure (0.206 pg/g). This suggests that a slight contamination has occurred during sampling or preparation. However, since concentrations in incubation solutions are systematically higher than in seawater blanks, we consider that contamination cannot account for the high Th concentrations in the incubation solutions. Data given in Table 3 are corrected for the chemical separation blank but not for this additional effect. Al concentrations (11.1–11.3 ng/g) in seawater blanks are 4–10 times higher than in Mediterranean seawater (Chou and Wollast, 1997) and incubation solutions are not systematically more concentrated than

Table 1
Al, Mn, Ba, Sr (ng/g) and REE concentrations (pg/g) in dissolved fractions

Sample	Time (h)	Al	Mn	Ba	Sr	La	Ce	Pr	Nd	Sm	Eu	Gd	Tb	Dy	Ho	Er	Tm	Yb	Lu	Ce anomaly
30 m																				
D0	0	11.6	3.6	23.3	8734	n.d.	n.d.	n.d.	n.d.	n.d.	n.d.	n.d.	n.d.	n.d.	n.d.	n.d.	n.d.	n.d.	n.d.	n.d.
D1	0	23.1	3.7	25.9	8917	5.10	6.99	0.97	4.51	1.22	n.d.	1.09	0.17	1.32	0.32	1.09	0.14	0.93	0.1	0.77
D2	6	10.0	4.4	27.5	8917	6.03	8.61	1.12	4.80	1.11	n.d.	1.10	0.17	1.23	0.30	1.02	0.12	0.85	0.1	0.81
D3	25	10.3	5.8	23.6	8960	6.55	8.91	1.31	6.27	1.51	n.d.	1.47	0.22	1.45	0.34	1.10	0.13	0.89	0.1	0.75
D4	51	7.8	5.2	23.6	8895	7.76	12.2	1.86	7.96	1.62	n.d.	1.70	0.25	1.64	0.38	1.18	0.14	0.93	0.1	0.80
D5.c[a]	70	10.2	5.7	28.3	9119	5.87	6.92	1.11	6.98	1.32	n.d.	1.30	0.20	1.40	0.30	1.05	0.12	0.76	0.1	0.66
D6	238	4.7	7.1	24.5	9122	16.8	20.2	2.69	11.7	2.61	n.d.	2.59	0.37	2.35	0.47	1.46	0.16	1.04	0.1	0.73
D7	504	9.4	4.6	23.6	9236	n.d.	n.d.	n.d.	n.d.	n.d.	n.d.	n.d.	n.d.	n.d.	n.d.	n.d.	n.d.	n.d.	n.d.	n.d.
D8	504	21.0	4.8	26.2	9133	19.1	13.6	3.16	13.6	2.9	n.d.	2.90	0.40	2.54	0.53	1.57	0.17	1.05	0.1	0.43
D9.c[a]	504	12.0	6.6	25.6	9060	4.50	5.41	0.84	4.15	1.1	n.d.	1.23	0.17	1.12	0.27	0.93	0.11	0.73	0.1	0.68
200 m																				
C0	0	16.4	2.5	16.0	8078	7.93	13.1	1.51	6.78	1.66	n.d.	1.45	0.24	1.68	0.46	1.45	0.23	1.28	0.3	0.93
C1	25	10.2	2.6	15.8	8165	7.75	12.0	1.29	6.30	1.45	n.d.	1.35	0.21	1.57	0.42	1.33	0.23	1.23	0.2	0.92
C2	27	10.4	2.7	17.4	8142	9.36	15.3	1.57	6.67	1.47	n.d.	1.24	0.20	1.61	0.41	1.38	0.19	1.20	0.2	0.97
C3	49	15.0	2.9	18.5	8166	5.97	11.1	1.15	5.33	1.29	n.d.	1.24	0.20	1.49	0.39	1.31	0.18	1.18	0.2	1.04
C4	241	10.4	3.4	25.8	8320	5.66	12.7	1.20	5.27	1.13	n.d.	1.11	0.16	1.35	0.29	1.14	0.03	0.91	n.d.	1.20
C5	481	8.6	3.5	18.9	8083	6.48	11.8	1.21	6.74	1.24	n.d.	1.25	0.17	1.44	0.30	1.13	0.03	0.94	n.d.	1.03
C6	481	13.1	3.5	22.2	8330	6.59	11.5	1.26	5.75	1.33	n.d.	1.26	0.18	1.52	0.32	1.21	0.04	1.02	n.d.	0.98
C7.c[b]	481	15.7	4.3	21.7	8330	11.8	27.6	2.87	12.4	3.09	n.d.	2.57	0.40	2.65	0.56	1.88	0.11	1.49	n.d.	1.17
Seawater Blanks																				
BL1		11.3	2.1	12.5	8225	3.81	4.28	0.82	3.94	1.57	n.d.	1.02	0.17	1.34	0.35	1.21	0.20	1.14	0.2	0.60
BL2		11.1	1.9	11.2	8277	4.18	4.02	0.81	3.91	1.48	n.d.	1.05	0.16	1.29	0.34	1.21	0.16	1.09	0.2	0.54

n.d. = Not determined.
[a] Irradiated sample.
[b] Poisoned with sodium azide.

Table 2
Al, Mn, Sr, Ba and REE concentrations of the particulate fraction in the incubation bottles (ng/g)

Sample	Time (h)	Al	Mn	Ba	Sr	La	Ce	Pr	Nd	Sm	Eu	Gd	Tb	Dy	Ho	Er	Tm	Yb	Lu	Ce anomaly	(La/Yb)n
30 m																					
D0	0	723	7.3	15.3	80.7	0.28	0.58	0.07	0.25	0.05	b.d	0.042	0.006	0.035	0.006	0.019	0.003	0.014	0.002	1.04	1.71
D1	0	971	10.2	19.6	123	0.36	0.75	0.09	0.34	0.06	b.d	0.054	0.009	0.051	0.010	0.028	0.005	0.028	0.004	1.04	1.13
D2	6	1254	9.6	16.8	41.1	0.35	0.87	0.08	0.32	0.06	0.01	0.050	0.007	0.042	0.008	0.023	0.003	0.019	0.003	1.30	1.58
D3	25	979	7.8	16.7	21.1	0.40	0.70	0.09	0.33	0.07	0.01	0.054	0.009	0.044	0.009	0.025	0.004	0.023	0.003	0.91	1.48
D4	51	845	7.9	15.1	13.5	0.36	0.61	0.08	0.30	0.05	0.01	0.046	0.008	0.044	0.008	0.022	0.004	0.020	0.003	0.88	1.55
D5.c[a]	70	1382	11.7	20.8	14.1	0.46	0.51	0.11	0.40	0.08	0.02	0.071	0.011	0.058	0.014	0.031	0.005	0.029	0.004	0.55	1.36
D6	238	724	4.5	12.6	9.9	0.26	0.49	0.06	0.21	b.d.	b.d	0.041	0.006	0.036	0.006	0.020	0.003	0.017	0.003	0.94	1.28
D7	502	815	7.3	14.4	9.0	0.28	0.68	0.06	0.22	0.04	b.d	0.036	0.006	0.041	0.010	0.021	0.004	0.018	0.004	1.25	1.30
D8	504	522	5.3	9.9	18.4	0.20	0.64	0.05	0.17	0.04	b.d	0.029	0.005	0.027	0.005	0.014	0.002	0.012	0.002	1.63	1.45
D9.c[a]	504	881	6.8	14.9	10.2	0.31	0.69	0.07	0.24	0.05	0.01	0.049	0.007	0.043	0.007	0.024	0.003	0.020	0.003	1.15	1.32
200 m																					
C0	0	113	2.76	12.4	15.4	0.15	0.38	0.01	0.06	b.d	b.d	b.d	b.d	b.d	b.d	b.d	b.d	b.d	b.d	1.82	n.d.
C1	25	105	2.33	9.2	9.21	0.07	0.58	0.01	0.05	b.d	b.d	b.d	b.d	b.d	b.d	b.d	b.d	b.d	b.d	5.03	n.d.
C2	27	132	3.52	13.7	13.2	0.08	0.44	0.01	0.06	b.d	b.d	b.d	b.d	b.d	b.d	b.d	b.d	b.d	b.d	3.42	n.d.
C3	49	65.5	1.78	7.1	7.27	0.05	0.11	0.01	b.d.	b.d	b.d	b.d	b.d	b.d	b.d	b.d	b.d	b.d	b.d	1.17	n.d.
C4	241	59.5	0.99	5.0	6.69	0.04	0.14	0.01	0.02	b.d	b.d	b.d	b.d	b.d	b.d	b.d	b.d	b.d	b.d	1.80	n.d.
C5	481	49.2	0.73	4.6	5.17	0.04	0.13	0.004	0.02	b.d	b.d	b.d	b.d	b.d	b.d	b.d	b.d	b.d	b.d	2.34	n.d.
C6	481	44.1	0.77	3.6	4.10	b.d.	b.d.	0.003	0.01	b.d	b.d	b.d	b.d	b.d	b.d	b.d	b.d	b.d	b.d	n.d.	n.d.
C7.c[b]	481	22.7	0.56	2.6	7.05	0.02	0.16	b.d.	b.d.	b.d	b.d	b.d	b.d	b.d	b.d	b.d	b.d	b.d	b.d	n.d.	n.d.
Blank		6.6	b.d.	0.1	2.46	0.01	0.15	b.d.	b.d.	b.d.	b.d.	b.d.	b.d.	b.d.	b.d.	b.d.	b.d.	b.d.	b.d.		

n.d. = Not determined, b.d. = below detection.
[a] Irradiated sample.
[b] Poisoned with sodium azide.

Table 3
Concentrations and isotopic ratios of Thorium isotopes

Sample	Time (h)	Particules			Solutions		
		^{232}Th (pg/g)	^{230}Th (10^{-6} pg/g)	^{230}Th/^{232}Th (10^{-6} mol/mol)	^{232}Th (pg/g)	^{230}Th (10^{-6} pg/g)	^{230}Th/^{232}Th (10^{-6} mol/mol)
30 m							
D0	0				0.53±0.03	3.1±3.0	5.80±5.6
D1	0	121±1	550±26	4.58±0.22	1.78±0.05	13.1±3	7.4±1.6
D2	12	131±1	576±110	4.45±0.85	n.d.	n.d.	n.d.
D3	24	108±1	517±41	4.82±0.39	0.83±0.04	4. 7±3.8	5.6±4.6
D4	48	124±2	575±40	4.69±0.34	0.43±0.04	10.8±7.7	25±18
D5[a]	68.2	89±5	385±240	4.39±2.7	0.59±0.03	3.8±1.4	6.5±2.5
D6	240	91±1	412±21	4.59±0.24	0.86±0.04	1.5±5.1	1.8±6
D7	504	95±1	400±24	4.26±0.27	0.26±0.03	2.7±1.6	10±6
D8	504	60±1	250±28	4.22±0.48	1.27±0.04	7.1±2.1	5.6±1.7
D9[a]	504	114±1	537±21	4.74±0.19	0.89±0.04	9.3±2.7	11±3
200 m							
C0	0	14.8±0.3	108±32	7.30±2.2	0.73±0.04	6. 8±1.1	9.3±1.6
C1	25	14.2±0.2	62±15	4.40±1.0	0.48±0.04	4.3±4.0	9.0±8.4
C2	25	n.d.	n.d.	n.d.	0.48±0.03	7.1±1.9	15±4
C3	49	8.9±0.3	n.d.	n.d.	0.42±0.03	3.6±1.0	8.6±2.6
C4	241	9.5±0.3	50±17	5.30±1.8	0.83±0.04	8.6±1.5	10±1.9
C5	481	4.08±0.08	26±8	6.40±1.9	0.45±0.03	4.1±0.9	9.2±2.0
C6	481	4.7±0.3	27±19	5.90±4.0	0.99±0.05	8.8±1.1	9.0±1.3
C7[b]	481	1.87±0.06	14±9	7.70±5.1	2.74±0.1	22.4±1.8	8.3±0.7
Seawater Blanks							
BL1	−24				0.27± 0.03	3.19±0.7	12±3
BL2	−24				0.33±0.02	3.4±3.1	10±9
200 m filtered water (analysis of 3 l)					0.206±0.008	3.38±0.4	13.6±1.8

n.d. = Not determined.
[a] Irradiated sample.
[b] Poisoned with sodium azide.

seawater blanks. Therefore, we suspect a strong contamination of the solutions with respect to Al (microbiologists wrapped their material and samples in Al foil to protect them from carbon contamination).

To compare our particulate matter concentrations with the literature, we express the quantity of element per mass of seawater (ng/g SW). Particulate Al concentrations in this work (0.16–0.42 ng/g SW at 30 m and 0.004–0.02 ng/g SW at 200 m) are of the same order of magnitude or slightly lower than previous measurements (0.05–0.6 ng/g SW) at the DYFAMED site (Sarthou and Jeandel, 2000). Particulate Ba concentrations (0.003–0.006 ng/g SW at 30 m and 0.0009–0.002 ng/g SW at 200 m) are lower than those determined in the Mediterranean Sea (0.169 ng/g SW at 50 m and 0.04–0.06 ng/g SW at 100–300 m) by (Dehairs et al., 1987b). In all cases, comparison is made with particles collected on filters with a much smaller pore size ($\approx 1\mu m$) compared to our work (60 μm), so that it is not surprising that we obtain different concentrations (there is no previously published data for these elements on large particles). The Nd concentrations in filtered large particles (> 50 μm) reported for the Sargasso Sea (0.03 pg/g SW at 40 m and 0.01 pg/g SW at 200 m, Jeandel et al., 1995) are in agreement with our values (0.035 pg/g SW at 30 m and 0.015 pg/g SW at 200 m).

4. Discussion

4.1. Particulate matter characteristics

The particulate matter is more abundant at 30 m than at 200 m. This is consistent with most biological activity occurring in the surface waters and eolian inputs. The elements in the particulate matter are enriched to various extents compared to crustal material. This is due to the addition of an authigenic fraction such as organic matter, biominerals, Mn oxyhydroxides precipitates or trace metal adsorption to the lithogenic material. Refractory elements such as Al and ^{232}Th are used as tracers of the lithogenic matter because they are expected to be insoluble in seawater and to present no authigenic enrichment. Nevertheless, Th isotopes raise the possibility of a small authigenic fraction of ^{232}Th (see Section 4.7). Similarly, the suggestion that Al is present in diatoms raises the possibility of nonlithogenic Al in the particulate matter (Hydes et al., 1988). Still, we consider that at this shallow coastal site, Al and Th should be mainly lithogenic and that using the bulk Al concentration to estimate the authigenic fraction of soluble elements will have a minor influence on the final result. The percentage of authigenic matter contributing to the total particulate matter, Fa, is given by:

$$\mathrm{Fa} = \left(1 - \left(\frac{\mathrm{X_c}}{\mathrm{Al_c}}\right)\left(\frac{\mathrm{Al_p}}{\mathrm{X_p}}\right)\right) \times 100 \qquad (1)$$

where X_c and Al_c are the average concentrations of the elements X and Al in the continental crust (Taylor and McLennan, 1985), X_p and Al_p are the concentrations of the elements X and Al in the particulate sample. Fa is larger at 200 m (95–99% for Sr, 92–94% for Ba, 50–70% for Mn, 20–37% for Nd) than at 30 m (57–97% for Sr, 49–68% for Ba, $\leq 30\%$ for Mn, $\leq 8\%$ for Nd). Lithogenic material of eolian origin accumulates in the surface waters before being carried through the water column by rapidly sinking particles (Ruiz-Pino et al., 1990). Therefore, its residence time at 200 m is much shorter than in the surface waters. This is why we collected less lithogenic material at 200 m compared to 30 m and why the relative contribution of the "local" authigenic matter is larger at 200 m compared to 30 m. In addition, aggregation between 30 m and 200 m of small particles enriched in authigenic component will dilute the lithogenic material. Specific processes may enhance this general trend: e.g. in surface waters, photo-reduction prevents the formation of Mn oxyhydroxides (Sunda et al., 1983). Lateral advection of particulate material at the sampling site is also possible but we cannot quantify it.

It is often assumed that the authigenic fraction is easily soluble (labile) while the lithogenic fraction is supposed to be refractory. However, recent works suggest that a substantial fraction of the lithogenic matter may be dissolved (Henry et al., 1994; Tachikawa et al., 1999a). We observe significant authigenic fractions on the residual particles for Mn and Ba. This suggests that a fraction of the authigenic material is not soluble under the conditions and on the timescale of the experiment.

4.2. Dissolution of tracers from the particulate matter

In order to remove the effect of heterogeneous distribution of particles among the different aliquots, we consider the percentage of dissolution (D_X) of an element (X) in the particulate matter rather than the concentration of this element in the incubation solutions or in residual particles, respectively. D_X is obtained by dividing the increase of concentration in solution by the total amount of element initially present on particles:

$$D_X = \left(\frac{X_s - X_{sw}}{X_s - X_{sw} + X_p} \right) \quad (2)$$

where X_s, X_p and X_{sw} are the concentrations of the element X in the incubation solution, on residual particles and in seawater blanks. Evolution of D_X as a function of time is shown on Fig. 2. We assume that the dissolution of the labile fraction of the element X on particles follows a first order kinetic law:

$$\left(\frac{dX_{p-labile}}{dt} \right) = -k_X X_{p-labile} \quad (3)$$

where $X_{p\text{-labile}}$ represents the concentration of labile particulate element X in the incubation sample. Eq. (3) is used as a proxy in many seawater–particle interaction models (Bacon and Anderson, 1982; Ruiz-Pino, 1994). From Eq. (3), we derive D_X as a function of time:

$$D_X(t) = D_X^{max}\left(1 - e^{\frac{(t+24)}{\tau_X}}\right) \quad (4)$$

and

$$D_X^{max} = \left(\frac{X_{p-labile}^{init}}{X_p^{init}} \right) \quad (5)$$

where t is the incubation time as defined previously, $\tau_X = 1/k_X$ is the residence time of element X on particles, D_X^{max} is the maximum dissolution fraction of X and the superscript init refers to the time of sample collection. We note that $X_p^{init} = X_s - X_{sw} + X_p$. The curves are fitted by eye by adjusting the values of τ_X and D_X^{max} (Fig. 2, Table 4). For Mn and Ce at 30 m, we suspect precipitation after 10 days of incubation so (1) we do not take D7 and D8 into account to adjust the curve and (2) we choose a value of D_X^{max} that is lower than D_X(20 days). For Al, D_{Al}^{max} is probably overestimated due to the contamination of the solution (see Section 3).

We obtain D_X^{max} values in agreement with the general knowledge about the behavior of these tracers and their relative solubility. At 30 m, D_X^{max} increases as follows: Th ($< 1.6\%$) $\approx$ Al ($< 2\%$) $<$ Heavy REE (0–4%) $<$ Light REE (5–7%) $<$ Mn (53%) $<$ Ba (60%) $<$ Sr (100%). At 200 m, the D_X^{max} increases as follows: Al ($< 6\%$) $<$ Th ($< 13\%$) $\approx$ Light REE (6–12%) $<$ Mn (80%) $\approx$ Ba (80%). For all the elements, D_X^{max} values are higher at 200 m than at 30 m because the proportion of insoluble lithogenic matter is lower at 200 m than at 30 m. This is in agreement with the higher $^{230}Th/^{232}Th$ ratio in the particulate matter from 200 m compared to 30 m (see Section 4.7). We obtain values for τ_X ranging from less than a day to more than 10 days. For Ba and Mn, the dissolution is faster at 30 m than at 200 m. In the case of Ce, the dissolution seems slower at 30 m than at 200 m (but the time constants are poorly constrained).

4.3. Refractory elements

Our study (Fig. 2 and Table 4) confirms the refractory nature of Al, Th and REE (Maring and Duce, 1987; Fisher et al., 1987; Greaves et al., 1994) and it justifies the use of Al and ^{232}Th as tracers of the particulate lithogenic matter. Compared to previous studies, the 30 m results demonstrate that Al, Th and REE, which are mainly lithogenic, remain insoluble even when strong bacterial activity occurs. At 200 m, the percentage of dissolution increases as a larger authigenic fraction is present on particulate matter.

4.4. Manganese

At 30 m and 200 m, 53% and 80% of the total particulate Mn is dissolved under biotic conditions (Fig. 2 and Table 4). The residence time (τ_{Mn}) is of the order of 3 days at 30 m and of the order of 5 days at 200 m. For both depths, the concentrations in

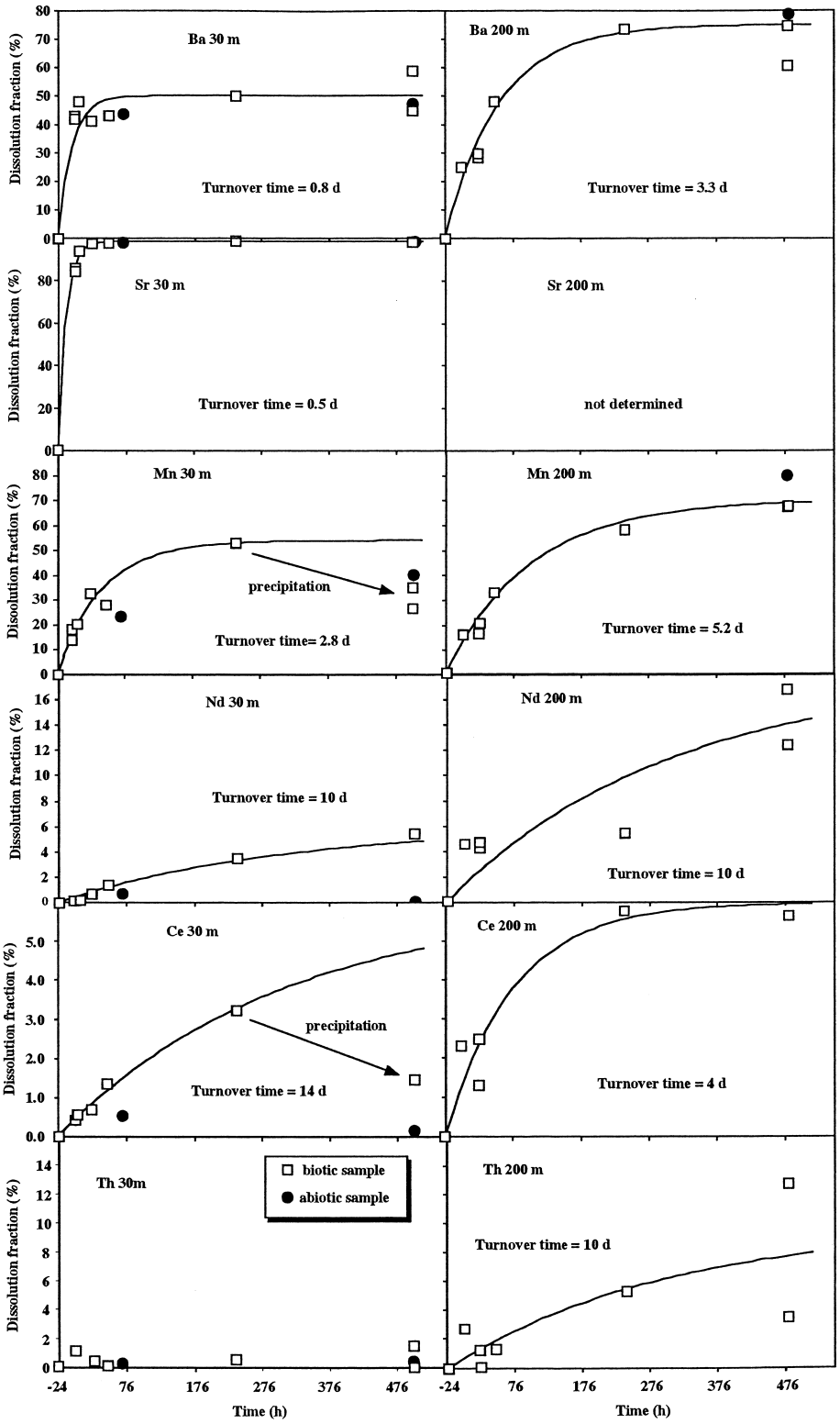

Fig. 2. Evolution of the percentage of dissolution (D_x) of Sr, Ba, Mn, Nd, Ce and Th as a function of time. The percentage of dissolution is given by Eq. (2). The curves represent the theoretical evolution of D_x with time assuming that dissolution follows a first order kinetics law (see Eq. (4)).

Table 4
Dissolution parameters

	Sr	Ba	Mn	La	Ce	Pr	Nd	Gd	Dy	Er	Yb	Al[a]	^{232}Th
30 m													
D_x^{max} (%)	99	50	53	7	3	5	5	6	4	3	-1[b]	≤ 2	≤ 1.6
T_x (days)	0.5	≤ 0.8	1.2	10	14	10	10	10	10	10	10	n.d.	
200 m													
D_x^{max} (%)		75	80	6	6	9	12	n.d.	n.d.	n.d.	n.d.	≤ 6	13
T_x (days)		3.3	5.2	1	4	1–10	1–10	n.d.	n.d.	n.d.	n.d.	n.d.	10

[a] D_{Al}^{max} is probably overestimated due to the contamination of the solution with Al foil (see Section 3).
[b] A negative value corresponds to a net adsorption/precipitation.

solution are higher in the sterilized samples than in the nonsterilized samples after 20 days of incubation (Table 1 and Fig. 2). At 30 m, we observe a decrease of D_{Mn} between 10 and 20 days whereas at 200 m dissolution continues over the same period. Under oxic conditions, the behavior of Mn is controlled by the balance between (1) oxidation of dissolved Mn^{2+} to Mn^{4+} as insoluble Mn oxides (Moffett, 1997) and (2) reduction of Mn oxides to Mn^{2+} by dissolved organic compounds (Sunda et al., 1983). The specific rate of Mn^{2+} bacterial oxidation in seawater k_{ox} is of the order of 1–2% per day (Moffett, 1997). The specific rate of Mn^{4+} reduction in seawater k_{red} is of the order of 20% per day but the value of k_{red} increases to 40% per day when 5 mg/l of marine humic substances where added (Sunda et al., 1983). Reduction is strongly enhanced by light but we do not consider this effect because our samples were kept in the dark during the incubation. It appears that the residence time of Mn on particles with respect to reduction of Mn^{4+} is $1/k_{red} = 2.5$–5 days which is close to our τ_{Mn} value.

What is the implication of this reversible process? If an element is subject to both dissolution and scavenging and if these processes both follow first order kinetics:

$$\left(\frac{dX_s}{dt}\right) = k_{-1}X_{p-labile} - k_1X_s \quad (6)$$

$$\left(\frac{dX_{p-labile}}{dt}\right) = -k_{-1}X_{p-labile} + k_1X_s \quad (7)$$

where k_1 is the scavenging rate, k_{-1} is the dissolution rate, X_s, X_l and X_p the concentrations in solution, of the labile particulate and of the total particulate. Then, we obtain by integration:

$$D_X(t) = D_X^{max}(1 - e^{-(k_1+k_{-1})(t+24)}) \quad (8)$$

with

$$D_X^{max} = \frac{\left(\frac{k_{-1}}{k_1+k_{-1}}\left(X_{sw} + X_{p-labile}^{init}\right) - X_{sw}\right)}{X_p^{init}} \quad (9)$$

If $k_1 \ll k_{-1}$, Eqs. (8) and (9) become equivalent to Eqs. (4) and (5) and the adjustment of the residence time based on our data will not change significantly when considering irreversible or reversible dissolution. This is the case for Mn where $k_1 = k_{ox} \ll k_{red} = k_{-1}$. If $k_1 \neq 0$ (scavenging occurs) then $D_X^{max} \leq X_{p-labile}^{init}/X_p^{init}$. In that case, Mn is constantly added to the particles so that a labile authigenic fraction remains on particles even after a long incubation time (this may be an alternative explanation for the significant Ba, Sr and Mn authigenic fraction found in residual particles). At steady state, we expect to obtain a ratio $Mn_s/Mn_{p-labile} = k_{-1}/k_1 \approx 10$–40. Therefore, more than 90% of the non-refractory Mn should be present in solution: this is consistent with our observations. Our experiments suggests dominance of reduction at least at the begining of the experiments. At 30 m, the decrease of D_{Mn} between 10 and 20 days suggests that oxidation becomes dominant over reduction at the end of the incubation.

Other experimental dissolutions of Mn have been proposed. Collier and Edmond (1984) studied particulate matter (mainly phytoplankton) collected from the Pacific Ocean. Their results ($D_{Mn}^{max} = 50\%$;

$\tau_{Mn} = 0.3$ day) agree with our values. These authors stressed the possible effect of filtration in breaking phytoplankton cells and the resulting artificial release of trace metals. Direct dissolution of aerosols (Saharan dust) in seawater yields comparable D_{Mn}^{max} (30%) but the process is much more rapid ($\tau_{Mn} \approx$ 0.003 day) (Guieu et al., 1994). This large timescale difference suggests that Mn is not present under the same chemical forms in the aerosols arriving in seawater and in the marine particles.

4.5. Barium and strontium

Particulate Sr is dissolved rapidly and extensively as expected if it is present as celestite (Bernstein et al., 1992). A significant fraction (20–30%) of the authigenic Ba is not dissolved during the experiment. This authigenic refractory fraction may be well crystallized barite ($BaSO_4$) that has a slow dissolution kinetics (Dehairs et al., 1980). At 30 m, the dissolution of Ba is less extensive but faster than at 200 m. The lower percentage of Ba dissolution of the 30 m particles can be related to their larger lithogenic fraction because this Ba may be present in poorly soluble minerals such as barite or silicates. The slower dissolution rate may be related to the more extensive crystallization of Ba at 200 m compared to 30 m: in the ocean barite is formed at depths around and below 200 m (Dehairs et al., 1980). The values obtained for τ_{Ba} (≤ 1 day at 30 m, 3 days at 200 m) are very short compared to the particulate Ba residence time of 24 years based on barite dissolution kinetics (Dehairs et al., 1980). This discrepancy suggests that in our samples, particulate Ba was not present as well-crystallized barite or that in the natural environment rapid particulate Ba dissolution is balanced by a rapid particle formation that did not occur in our experiment.

The faster Ba dissolution in the 30 m experiment compared to the 200 m experiment is also consistent with the faster mineralization of POC and the larger bacterial production (Yoro, 1998). For the 30 m samples, small pteropods were present on the first filters (D0–D4) and for irradiated samples (D5–D9) and were absent on the last ones (D6–D8). Dissolution of the pteropod shells ($CaCO_3$) may provide a substantial source of labile Ba and Sr. Additional release of Ba and Sr may come from the dissolution of coccoliths. The pH and the inorganic carbon of the solutions were not measured so that it is not possible to determine precisely the influence of CO_2 release on the dissolution of carbonates. However, about 460 μM C (at 200 m) and 720 μM C (at 30 m) of TOC were consumed by bacteria in the incubation bottles (Yoro, 1998). Then, 244 μM of CO_2 at 200 m and 421 μM of CO_2 at 30 m could have been produced during the experiment (corresponding to bacterial growth efficiency of 40–50%) and could have acidified the solution. Dissolution of $CaCO_3$ will tend to buffer the pH of the solution.

The effect of $CaCO_3$ dissolution can be estimated from the observation of the incubated material in the 30-m experiment where the largest carbon mineralization occurs (Table 5). After 20 days of incubation pteropod shells were completely dissolved whereas some coccoliths were still visible. This suggests that the final incubation solutions are undersaturated with respect to aragonite but that calcite still buffers the solution. It implies that $CO_3^{2-} \sim 40$–60 μM (Copin-Montégut, 1996). Considering that at the end of the incubation $\Sigma CO_2 \sim 2400$ μM, it follows that pH ~

Table 5
Initial seawater and final incubation solution estimated compositions

	Initial seawater	D7 and D8
ΣCO_2 (μM)	2000	2400[a]
HCO_3^- (μM)	1650	2260
CO_3^{2-} (μM)	345	40–60
pH(SWS)	8.2	7.2–7.4
Total PO_4^{3-} (μM)	0.1	3.3[b]
Fraction of La as La^{3+}–CO_3^{2-}-complexes[c]	91%	53%
Fraction of La as free La^{3+}[c]	4%	21%
Fraction of La as La^{3+}–SO_4^{3-}-complexes[c]	3%	17%
Fraction of La as La^{3+}–PO_4^{3-} complexes[c]	0.3%	2%

[a] Estimated assuming that $\Sigma CO_2 = \Sigma CO_2$ (seawater) + 400 μM.

[b] Estimated from TOC mineralization assuming a P/C Redfield ratio of 1/120.

[c] Speciation of the dissolved REE was calculated by taking into account free REE as well as chloride, fluoride, sulfate, carbonate, bicarbonate and phosphate complexes (Byrne and Sholkovitz, 1996).

7.2–7.4. This unusually low pH is due to the combination of the strong carbon mineralization (generally found in cold deep waters) and of the high temperature. Therefore, the high POC content of the incubation solutions may have controlled the dissolution process. Such a control may not be as efficient in real seawater. However, such conditions may exist in micro-environments when particulate matter is being degraded.

4.6. Fractionation between REE

Dissolved REE are scavenged by oxygen-donor substance such as Mn–Fe oxyhydroxides and particulate organic matter (Balistrieri et al., 1981; Sholkovitz et al., 1994; Tachikawa, 1999). The scavenged REE are redissolved at greater depths by the remineralization of carrier particles. These processes induce fractionations between the different REE in both dissolved and particulate fractions (Tachikawa et al., 1999a). Fig. 3 presents shale-normalized REE patterns of the incubation solutions at 30 m. During the incubation, the concentrations of dissolved Light REE (LREE: La, Ce, Pr, Nd) increase whereas those of dissolved Heavy REE (HREE: Dy, Ho, Er, Tm, Yb, Lu) slightly decrease (Fig. 3a). In natural environments, authigenic LREE are enriched on particles compared to HREE (Byrne and Sholkovitz, 1996; Tachikawa et al., 1999b). Therefore, when dissolution of particulate REE occurs, LREE are more abundantly released to the solution than HREE. Our results are in good agreement with field observations of the preferential LREE release by river particles (Sholkovitz, 1992) and with the REE patterns of sequentially leached marine particles (Sholkovitz et al., 1994; Tachikawa et al., 1997). Fig. 2 presents D_{Nd} and D_{Ce} as a function of time. At 200 m, both D_{Nd} and D_{Ce} are twice higher than at 30 m (Table 4). At both depths, τ_{Nd} is estimated around 10 days. τ_{Ce} is shorter at 200 m (4 days) than at 30 m (14 days). Recently, Tachikawa et al. (1999b) demonstrated that the negative Ce anomaly of seawater samples is formed by two processes: (1) microbially mediated in situ Ce oxidation (Ce oxide is insoluble, Elderfield, 1988; Moffett, 1990) and (2) preferential dissolution of Ce neighbors which increases a relative depletion of Ce. The higher dissolution of La, Pr or Nd compared to Ce observed during the incubation confirms this mechanism. For the 30 m samples, there is a simultaneous precipitation of Ce and Mn in the biotic samples that is not observed for Nd. Our results are consistent with the mechanism suggested by Moffett (1990): the oxidation of Ce III to Ce IV is coupled to the microbially mediated oxidation of Mn II to Mn IV. This coupling does not affect Nd (present only as Nd III).

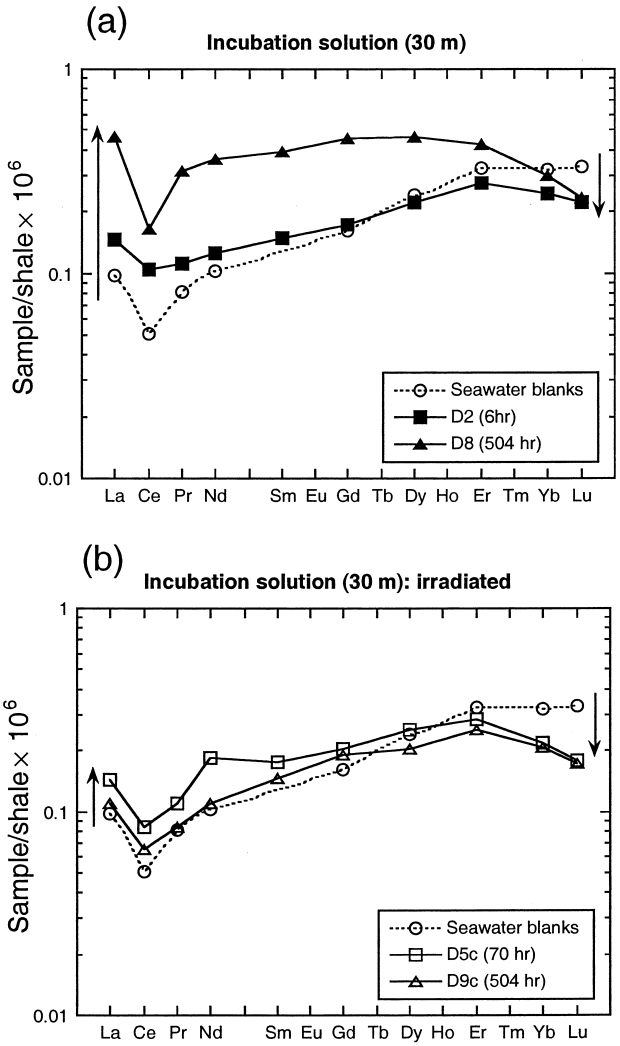

Fig. 3. Shale normalized REE patterns of the incubation solutions at 30 m: (a) nonirradiated samples and (b) irradiated samples. The trends of concentration variations of LREE and HREE are indicated by upwards and downwards arrows.

The behavior of REE in seawater is strongly controlled by REE–CO_3^{2-} complexes that stabilize REE in solution with a stronger effect on HREE compared to LREE (Byrne and Sholkovitz, 1996). We estimated the speciation of La for the initial

seawater and for D8 (Table 5). Due to the strong decrease in CO_3^{2-} during the incubation, carbonate complexes represent only 53% of the dissolved La in the final incubation solution whereas 91% of the La was present as carbonate complexes in the initial seawater. The increase of dissolved REE when the pH decreases is consistent with previous observations in natural waters (Gaillardet et al., 1997). The REE pattern in the final incubation solution depends on the REE pattern of the initial seawater and of the labile REE on the incubated particles, on the REE fractionation during sorption on Fe–Mn oxyhydroxides and organic matter and during phosphate precipitation if it occurred. Due to the large number of unconstrained parameters, we did not try to reconstruct it.

In the 30 m incubation solutions, the increase of LREE concentrations is much smaller for the irradiated samples (D5c and D9c in Fig. 3b) than for the biotic samples. It suggests that the LREE dissolution is enhanced by biotic processes. By contrast, the HREE precipitation may be related to an abiotic process since both irradiated and non-irradiated samples show similar decreases of concentration.

4.7. Dissolution of Th isotopes

Thorium is a very insoluble element. ^{232}Th and ^{230}Th have distinct sources in the ocean (Roy-Barman et al., 1996). ^{232}Th is derived from continental material. ^{230}Th is present in lithogenic matter but in the marine environment, it is also produced by the in situ radioactive decay of ^{234}U in seawater and rapidly scavenged by particulate matter. The production of ^{230}Th at a known rate is used to calibrate scavenging and marine particle transport models (Bacon and Anderson, 1982). One of the most important outcomes of these ^{230}Th studies is that the scavenging of particle reactive metals is reversible.

The ^{230}Th/^{232}Th ratio can be used to estimate the fraction α of authigenic Th in the particles:

$$\alpha = \frac{R_p - R_{litho}}{R_{sw} - R_{litho}} \quad (10)$$

where R represents the ^{230}Th/^{232}Th ratio, the subscript p, litho and sw correspond to particles, lithogenic material and seawater, respectively, $R_{litho} = 4.4 \times 10^{-6}$ (Andersson et al., 1995) and $R_{sw} = 13.6 \times 10^{-6}$ (Table 3). At 30 m, $R_p \leq 4.8 \times 10^{-6}$ so that $\alpha \leq 4\%$. At 200 m, $R_p \approx 5\text{–}6 \times 10^{-6}$ so that $\alpha \approx 6\text{–}17\%$. This increase of α with depth is consistent with the uptake of dissolved Th on the particles during their transit from 30 m to 200 m (Roy-Barman et al., 2000).

During the incubations, there is a significant increase of dissolved Th. This increase may represent the total quantity of Th that can be potentially released from the particles or it may only represent the net effect between dissolution of particulate matter and scavenging by the residual particles. We can use Th isotopes to investigate the details of these processes. We take advantage of the fact that marine particles and the seawater in which they are diluted have distinct ^{230}Th/^{232}Th ratios: particulate Th (^{230}Th/^{232}Th $= 4.5 \times 10^{-6}$ at 30 m and ^{230}Th/^{232}Th $= 5\text{–}6 \times 10^{-6}$ at 200 m) contains a large fraction of lithogenic Th (^{230}Th/^{232}Th $= 4\text{–}5 \times 10^{-6}$) and dissolved Th is enriched in ^{230}Th due to the in situ production (^{230}Th/^{232}Th $= 1.36 \times 10^{-5}$). Fig. 4 presents the ^{230}Th/^{232}Th ratio versus $1/^{232}$Th for the incubation solutions. In the case of a simple binary mixing (Th in incubation solution = seawater Th + particle derived Th due to dissolution), ^{230}Th/^{232}Th ratio as a function of $1/^{232}$Th for the incubation solutions is given by:

$$R_s = \frac{C_{sw} R_{sw} - C_p R_p}{C_{sw} - C_p} + C_{sw} C_p \frac{R_p - R_{sw}}{C_{sw} - C_p} \frac{1}{C_s} \quad (11)$$

where C_s and C_{sw} are the ^{232}Th concentrations in the incubation solution and seawater blank, C_p is amount of ^{232}Th dissolved from particles divided by the mass of the incubation solution and R_s, R_{sw} and R_p are the ^{230}Th/^{232}Th ratios in the incubation solution, seawater blank and particles (we consider that dissolution of particulate matter does not change significantly the mass of the incubation solution). Therefore, the incubation solutions should lie on a straight line between marine particles and seawater blanks (Fig. 4a). If readsorption occurs, concentration will decrease but there will be no change of ^{230}Th/^{232}Th ratio so that the sample will be shifted horizontally toward the right. If there is a rapid reversible equilibrium between seawater and particles, we

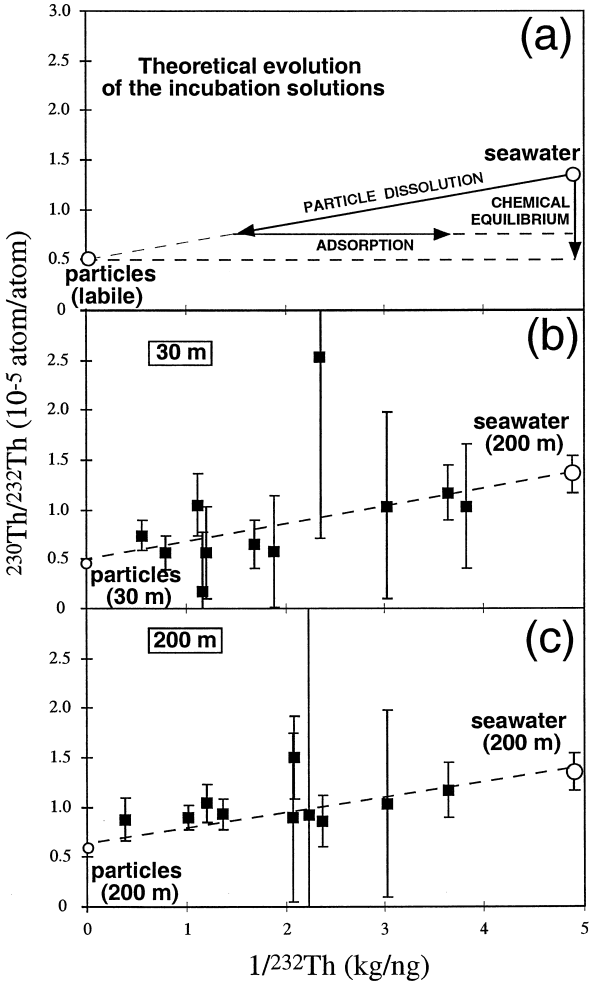

Fig. 4. $^{230}Th/^{232}Th$ ratio versus $1/^{232}Th$ for the incubation solutions. (a) Theoretical evolution of the incubations solutions: (1) for simple dissolution, incubation solutions lie on a straight line between labile marine particles and seawater blanks; (2) if readsorption occurs the sample will be shifted horizontally toward the right; (3) for rapid reversible equilibrium between seawater and particles, incubation solutions lie on a straight vertical line (see text for details). (b) 30 m data. (c) 200 m data. The 30 m and 200 m data can be explained by simple dissolution or simple dissolution + readsorption but rapid reversible equilibrium between seawater and particles can be ruled out. The straight lines passing through the incubation solutions, the initial seawater and the bulk particles indicate that the bulk particles represent a possible Th source during the simple dissolution of the particulate matter in seawater. However, it is also possible to draw straight lines passing through the incubation solutions, the initial seawater and ending up significantly above the bulk particles, leaving open the possibility that the $^{230}Th/^{232}Th$ ratio of the labile fraction is distinct from the $^{230}Th/^{232}Th$ ratio of the bulk particles.

expect no change of concentrations and the isotopic ratio of the incubation solution will be buffered by the $^{230}Th/^{232}Th$ ratio of marine particles because they contain the majority of Th. The data can be explained by simple dissolution or simple dissolution + readsorption (Fig. 4b and c) but rapid reversible equilibrium between seawater and particles can be ruled out.

The $^{230}Th/^{232}Th$ ratio of the incubation solutions points towards the $^{230}Th/^{232}Th$ ratio of the labile fraction of the particles. On Fig. 4b and c, the straight lines passing through the incubation solutions, the initial seawater and the bulk particles indicates that the bulk particles represent a possible Th source during the simple dissolution of the particulate matter in seawater. In this case, labile and bulk Th cannot be distinguished isotopically. However, it is also possible to draw straight lines passing through the incubation solutions and the initial seawater, ending up significantly above the bulk particles. This leaves open the possibility that the $^{230}Th/^{232}Th$ ratio of the labile fraction is distinct from the $^{230}Th/^{232}Th$ ratio of the bulk particles.

The small shift between the seawater blanks and the 200 m seawater is consistent with a small amount of contamination of the blanks by crustal material, but it will not change the global correlation obtained for the incubation solutions and the 200 m seawater. It is surprising to obtain an irreversible dissolution for Th because it is a very insoluble element and there is a high particle concentration. However, the degradation of particulate matter may produce a large amount of colloidal matter. These colloids scavenge Th (Baskaran et al., 1992) but due to their small size they remain in "solution" during the filtration, producing these apparently high dissolved Th concentrations.

4.8. Is there a link between inorganic tracers and organic matter dissolution?

In principle, the influence of biological activity on inorganic tracer behavior should lead to distinct tracer concentrations in sterilized and non sterilized dissolved samples. However, since the samples were sterilized 24 h (200 m samples) to 48 h (30 m samples) after particle collection at sea, significant concentration changes under biotic conditions may have occurred before the sterilization. For Ba and Sr at 30 m, dissolution occurred before sterilization so

that we have no clue whether it is biotic or abiotic. For Ba at 200 m, the lack of significant difference between samples C6 (biotic) and C7 (poisoned) suggests that an abiotic process controls dissolution. For Mn at 30 and 200 m, both concentrations and D_{Mn} are significantly higher for poisoned or irradiated samples (C7, D9) compared to biotic samples (C5–C6, D7–D8), suggesting a biotic control on the reprecipitation of Mn. This process may also control the simultaneous precipitation of Ce. We noted in Section 4.6 that LREE dissolution is enhanced by biotic processes and that HREE precipitation may be related to abiotic processes. At 200 m, REE and Th concentrations are much higher in C7 (poisoned) than in C5 and C6 (not poisoned). This is not due to sample contamination by sodium azide addition. Still, it is not clear if this difference is just due to the lack of biological activity in C7 (this would imply that biological activity has a very strong influence on the scavenging of these elements and this was not observed at 30 m) or to sodium azide inducing a larger extent of REE and Th release (for an unknown reason). We noted that during these experiments, POC oxidation occurs on timescales of the same order as inorganic tracers (Yoro, 1998) and we suggested earlier that POC oxidation to CO_2 may trigger the dissolution of some inorganic phases. The high enrichment of POC in the incubation bottles compared to natural environments enhanced the amount of CO_2 released and the rate of pH change. Therefore, it may have produced artificially high D_X and τ_X values compared to seawater. However, both D_X and τ_X derived from the incubation may be relevant for micro-environment in which particulate matter is degraded. This is particularly interesting with regards to the recent claim that a biologically mediated dissolution of calcium carbonate occurs above the chemical lysocline (Milliman et al., 1999). It was recently suggested that bacterial dissolution of the organic coating of diatom frustules can enhance the dissolution of silica (Bidle and Azam, 1999). Bacterial dissolution of organic coating may also enhance dissolution of some of the tracers presented in this work: (1) it removes a protective coating from mineral phases and (2) organic coatings are potential carriers of particle reactive metals such as REE (Balistrieri et al., 1981; Sholkovitz et al., 1994; Tachikawa et al., 1999a).

5. Conclusion

Inorganic tracers display a wide range of solubilities during the degradation of large marine particles. These variations are in agreement with the general knowledge concerning these tracers in the ocean. There are also significant variations in the timescales necessary to achieve this dissolution. These timescales range from less than one day to 14 days. For Mn, the timescale that we obtain is grossly consistent with previous estimates whereas for Ba, the timescale that we obtain is much shorter than what is inferred from dissolution kinetics considerations. We suspect that during the experiment, biological activity has a significant control on the dissolution process. This control may be due in part to the high particulate matter content of the incubation solutions. Therefore, in future studies, an effort should be made to work with less particle-enriched environments. However, this work stresses the possibility of rapid dissolution of inorganic tracers in confined environments.

Acknowledgements

We are grateful to J.C. Marty for his support to our project at the DYFAMED station. We thank the captain and the crew of the R.V. Professeur Georges Petit for their assistance and hospitality during the cruise. We thank C. Bournot-Marrec, M. Goutx, F. Van Wambeke, P. Brunet, M. Valladon, B. Reynier, L. Guidi for their help at different stages of the project. We are grateful to F. Dehairs, R. Sherrell and two anonymous reviewers for their fruitful comments. The thesis of R.A.-M. was partly financed by the "Conselho Nacional de Pesquisa do Brasil (CNPq)" and by the "Société de Secours des Amis des Sciences".

References

Andersson, P.S., Wasserburg, G.J., Chen, J.H., Papanastassiou, D.A., Ingri, J., 1995. ^{238}U–^{234}U and ^{232}Th–^{230}Th in the Baltic sea and in river water. Earth Planet. Sci. Lett. 130, 217–234.

Bacon, M.P., Anderson, R.F., 1982. Distribution of thorium isotopes between dissolved and particulate forms in the Deep-Sea. J. Geophys. Res. 87, 2045–2056.

Balistrieri, L., Brewer, P.G., Murray, J.W., 1981. Scavenging residence times of trace metals and surface chemistry of sinking particles in the deep ocean. Deep-Sea Res. 28, 101–121.

Banner, J.L., Wasserburg, G.J., Chen, J.H., Moore, C.H., 1990. ^{234}U–^{238}U–^{230}Th–^{232}Th systematics in saline groundwaters from central Missouri. Earth Planet. Sci. Lett. 101, 296–312.

Baskaran, M., Santschi, P.H., Benoit, G., Honeyman, B.D., 1992. Scavenging of thorium isotopes by colloids in seawater of the Gulf of Mexico. Geochim. Cosmochim. Acta 56, 3375–3388.

Bernat, M., Church, T., Allègre, C.J., 1972. Barium and strontium concentrations in Pacific and Mediterranean sea water by direct isotope dilution mass spectrometry. Earth Planet. Sci. Lett. 16, 75–80.

Bernstein, R., Bernstein, H., Bernstein, B.R., Betzer, P.R., Greco, A.M., 1992. Morphologies and transformations of celestite in seawater: the role of acantharians in strontium and barium geochemistry. Geochim. Cosmochim. Acta 36, 3273–3279.

Bidle, K.D., Azam, F., 1999. Accelerated dissolution of diatom silica in marine bacterial assemblages. Nature 397, 508–512.

Byrne, R.H., Sholkovitz, E.R., 1996. Marine chemistry and geochemistry of the lanthanides. In: Gschneider, K.A. Jr., Eyring, L. (Eds.), Handbook on the Physics and Chemistry of Rare Earths. Elsevier.

Chen, J.H., Edwards, R.L., Wasserburg, G.J., 1987. ^{238}U–^{234}U and ^{232}Th in seawater. Earth Planet. Sci. Lett. 80, 241–251.

Chou, L., Wollast, R., 1997. Biogeochemical behavior and mass balance of dissolved aluminum in the western Mediterranean Sea. Deep-Sea Res. 44, 741–768.

Collier, R.W., Edmond, J.M., 1984. The trace element geochemistry of marine biogenic particulate matter. Prog. Oceanogr. 13, 113–199.

Copin-Montégut, G., 1996. Chimie de l'eau de mer. Institut Océanographique, Paris, 320p.

Davies, J.E., Buat-Ménard, P., 1990. Impact of atmospheric deposition on particulate manganese and aluminum distribution in northern Mediterranean surface water. Palaeogeogr., Palaeoclimatol., Palaeoecol. 89, 35–45.

Dehairs, F., Chesselet, R., Jedwab, J., 1980. Discrete suspended particles of barite and the barium cycle in the open ocean. Earth Planet. Sci. Lett. 49, 528–550.

Dehairs, F., Goeyens, L., 1987. Dissolved barium and nutrients in the Southern Ocean: their potential use as tracers for the characterization of the different watermasses. Belgian National Colloquium on Antarctic Research. Ed. Science Policy Office.

Dehairs, F., Lambert, C.E., Chesselet, R., Risler, N., 1987b. The biological production of marine suspended barite and the barium cycle in the Western Mediterranean Sea. Biogeochemistry 4, 119–139.

Elderfield, H., 1988. The oceanic chemistry of the Rare Earth Elements. Philos. Trans. R. Soc. London, Ser. A 325, 105–126.

Fisher, N.S., Teyssié, J.-L., Krishnaswami, S., Baskaran, M., 1987. Accumulation of Th, Pb, U and Ra in marine phytoplankton and its geochemical significance. Limnol. Oceanogr. 32, 131–142.

Fowler, S.W., Buat-Ménard, P., Yokohama, Y., Ballestra, S., Holm, E., Van Nguyen, H.V., 1987. Rapid removal of Chernobyl fallout from Mediterranean surface waters by biological activity. Nature 329, 56–58.

Francois, R., Honjo, S., Manganini, S.J., Ravizza, G.E., 1995. Biogenic barium fluxes to the deep sea: implications for paleoproductivity reconstruction. Global Biogeochem. Cycles 9, 289–303.

Gaillardet, J., Dupré, B., Allègre, C.J., Negrel, P., 1997. Chemical and physical denudation in the Amazon River Basin. Chem. Geol. 142, 141–173.

Greaves, M.J., Rudnicki, M., Elderfield, H., 1991. Rare Earth Elements in the Mediterranean Sea and mixing in the Mediterranean outflow. Earth Planet. Sci. Lett. 103, 169–181.

Greaves, M.J., Statham, P.J., Elderfield, H., 1994. Rare earth element mobilization from marine atmospheric dust into seawater. Mar. Chem. 46, 255–260.

Guerzoni, S., Molinaroli, E., Chester, R., 1997. Saharan dust inputs to the western Mediterranean Sea: depositional patterns, geochemistry and sedimentological implications. Deep-Sea Res. 44, 631–654.

Guieu, C., Duce, R.A., Arimoto, R., 1994. Dissolved input of manganese in the ocean: the aerosol source. J. Geophys. Res. 99, 18789–18800.

Henry, F., Jeandel, C., Minster, J.-F., 1994. Particulate and dissolved Nd in the Western Mediterranean Sea: sources, fates and budget. Mar. Chem. 45, 283–305.

Heussner, S., Rati, C., Carbonne, J., 1990. The PPS3 time-series sediment trap and the trap sample processing techniques used during the ecomarge experiment. Cont. Shelf Res. 10, 943–958.

Hydes, D.J., De Lange, G.J., De Baar, H.J.W., 1988. Dissolved aluminum in the Mediterranean. Geochim. Cosmochim. Acta 52, 2107–2114.

Jeandel, C., Bishop, J.K., Zindler, A., 1995. Exchange of Nd and its isotopes between seawater small and large particles in the Sargasso Sea. Geochim. Cosmochim. Acta 59, 535–547.

Kirchman, D.L., Keil, R.G., Simon, M., Welshmeyer, N.A., 1993. Biomass and production of heterotrophic bacterioplankton in the oceanic subarctic Pacific. Deep-Sea Res. 40, 967–988.

Lal, D., 1977. The oceanic microcosm of particles. Science 198, 997–1009.

Landing, W.M., Bruland, K.W., 1987. The contrasting biogeochemistry of iron and manganese in the Pacific Ocean. Geochim. Cosmochim. Acta 51, 29–43.

Maring, H.B., Duce, R.A., 1987. The impact of atmospheric aerosols on trace metal geochemistry in open ocean surface seawater: I. Aluminium. Earth Planet. Sci. Lett. 84, 381–392.

McCave, I.N., 1975. Vertical fluxes of particles in the ocean. Deep-Sea Res. 22, 491–502.

Milliman, J.D., Troy, P.J., Balch, W.M., Adams, A.K., Li, H.Y., Mackenzie, F.T., 1999. Biologically mediated dissolution of calcium carbonate above the chemical lysocline? Deep-Sea Res. 46, 1653–1669.

Moffett, J.W., 1990. Microbially mediated cerium oxidation in sea water. Nature 345, 421–423.

Moffett, J.W., 1994. A radiotracer study of cerium and manganese up take onto suspended particles in Chesapeake Bay. Geochim. Cosmochim. Acta 58, 695–703.

Moffett, J.W., 1997. The importance of microbial oxidation in the upper ocean: a comparison between the Sargasso Sea and equatorial Pacific. Deep-Sea Res. 44, 1277–1291.

Morley, N.H., Burton, J.D., Tankere, S.P.C., Martin, J.M., 1997. Distribution and behaviour of some dissolved trace metals in the Western Mediterranean Sea. Deep-Sea Res. 44, 675–691.

Murnane, R.J., Cochran, J.K., Sarmiento, J.L., 1994. Estimate of particle- and thorium-cycling rates in the northwest Atlantic Ocean. J. Geophys. Res. 99, 3373–3392.

Porter, K.G., Feig, Y.S., 1980. The use of DAPI for identifying and counting aquatic microflora. Limnol. Oceanogr. 25, 943–948.

Roy-Barman, M., Chen, J.H., Wasserburg, G.J., 1996. ^{230}Th–^{232}Th systematics in the Central Pacific Ocean: the sources and the fates of thorium. Earth Planet. Sci. Lett. 139, 351–363.

Roy-Barman, M., Coppola, L., Souhaut, M., 2000. Thorium isotopes in the Western Mediterranean Sea: an insight into the marine particle dynamics. Deep-Sea Res. Submitted for publication.

Ruiz-Puno, D.P., 1994. Modèle Colume d'eau au site DYFAMED. In Rabouille, C. (Ed.), Modelisation des cycles biogeochimiques marins: application aux opèrations de JGOFS-France, Atelier 1993, Rapport No. 18.

Ruiz-Pino, D.P., Lambert, C.E., Jeandel, C., Buat-Ménard, P., 1990. Modelling the biogenic transport of atmospheric particles in the Mediterranean Sea. Global Planet. Change 3, 47–65.

Sarthou, G., Jeandel, C., 2000. Seasonal variations of iron concentrations in the Ligurian Sea and iron budget in the western Mediterranean Sea. Mar. Chem., accepted for publication.

Schaffer, G., 1996. Biogeochemical cycling in the global ocean: 2. J. Geophys. Res. 101, 3723–3735.

Sempéré, R., Yoro, S.C., Van Wambeke, F., Charrière, B., 2000. Microbial decomposition of large organic particles in the northwestern Mediterranean Sea. An experimental approach. Mar. Ecol.: Prog. Ser. 198, 61–72.

Sholkovitz, E.R., 1992. Chemical evolution of Rare Earth Elements: fractionation between colloidal and solution phases of filtered river water. Earth Planet. Sci. Lett. 114, 77–84.

Sholkovitz, E.R., Landing, W.M., Lewis, B.L., 1994. Ocean particle chemistry: the fractionation of Rare Earth Elements between suspended particles and seawater. Geochim. Cosmochim. Acta 58, 1567–1579.

Sunda, W.G., Huntsman, S., Harvey, G.R., 1983. Photoreduction of manganese oxides in seawater and its geochemical and biological implications. Nature 301, 234–236.

Tachikawa, K., Jeandel, C., Dupré, B., 1997. Distribution of Rare Earth Elements and neodymium isotopes in settling particulate material of the tropical Atlantic Ocean (EUMELI site). Deep-Sea Res. 44, 1769–1792.

Tachikawa, K., Jeandel, C., Roy-Barman, M., 1999a. A new approach to Nd residence time in the ocean: the role of atmospheric inputs. Earth Planet. Sci. Lett. 170, 433–446.

Tachikawa, K., Jeandel, C., Vangriesheim, A., Dupré, B., 1999b. Distribution of Rare Earth Elements and neodymium isotopes in suspended particles of the tropical Atlantic Ocean (EUMELI site). Deep-Sea Res. 46, 733–756.

Taylor, S.R., McLennan, S.M., 1985. The Continental Crust: Its Composition and Evolution. Blackwell.

Valladon, M., Dupré, B., Polvé, M., 1995. ICP-MS chemical analysis of geological samples: a new method for interferences and shifts corrections. Application to REE determination. EUG8 Strasbourg, Terra abstracts supplement 1 to Terra Nova 7 347.

Yoro, S.C., 1998. Décomposition de la matière organique et du flux de carbone à travers le compartiment bactérien en milieu marin. thèse, Aix-Maseille II.